Desalination and Water Treatment
www.deswater.com

doi: 10.5004/dwt.2021.27659

235 (2021) 26–38
September

Exergetic and thermo-economic analysis of different multi-effect configurations powered by solar power plants

Y. Aroussy*, D. Saifaoui, A. Lilane

Laboratory of Renewable Energies and Dynamics of Systems, Hassan II University, Faculty of Science Aîn Chock, El-Jadida Road Km9-BP 5366 Maarif Casablanca-Morocco, Tel. +212 (0) 673-697-179; emails: aroussy110@gmail.com (Y. Aroussy), ddsaifaoui@gmail.com (D. Saifaoui), m.amine.lilane@gmail.com (A. Lilane)

ABSTRACT

The increasing urbanization and population growth that humanity has undergone in the last century constitutes a real challenge for our ecosystem and our economic model. Energy needs and consumption of natural resources like water continue to increase year after year. One of the possible solutions is seawater desalination using renewable energies. This study presents exergy and thermo-economic analyses of different multi-effect distillation (MED) configurations. Our systems are powered by thermal energy produced in solar concentration units at parabolic trough collector. Therminol VP-1 oil is used as a heat transfer fluid for indirect steam generation through the solar field and the evaporator heat exchanger. The comparisons made relate to a nominal production of 350 m^3/d of distilled product. The results reveal that for the MED-PF (parallel/crossfeed) configuration, the total price of water is 1.44 \$/m^3 which is less expensive than the other configurations, MED-FFH (forward feed configuration with feedwater heaters), MED-BF (backward feed) and MED-FF (forward feed) of approximately –21.9%, –21.4% and –42.6%. In addition, the specific energy consumption (STPC, kWh/m^3) of a MED-PF configuration is significantly better with more than 74% of energy saving. Moreover, its performance becomes better if we increase the number of effects to more than 12 effects.

Keywords: Desalination; Electricity–water cogeneration; Multi-effect distillation; Thermo-economic; Rankine cycle

1. Introduction

Due to population growth and changing climatic conditions, many problems around the world will be caused by drought [1,2]. However, most of the countries located in the Mediterranean region have abundant seawater resources and an excellent level of solar radiation.

The use of renewable energies instead of conventional fossil fuels can be an effective means of increasing the production capacity of desalinated water, at an attractive cost [3]. Experts recognize the great potential of desalination of seawater by solar thermal energy. Indeed, several methods are possible, the connection of a MED thermal desalination system (multi-effect distillation) with a concentrated thermal solar source (CSP) remains one of the most used [4]. This system is characterized by its low energy consumption compared to the multistage flash system [5].

Supplying MED with low temperature steam (around 65°C) significantly reduces its energy consumption, which makes it more and more competitive. Recent developments in solar thermal collectors have enabled MED-assisted desalination to compete technically and economically with conventional desalination systems. Indeed, MED demonstration units with solar assistance obtained higher performances [6,7].

The performance of a MED desalination plant can be optimized by coupling it to thermal or mechanical vapor compression systems (TVC or MVC). Each of these two systems (TVC and MVC) has its own advantages. One of the main advantages of the TVC system is the recycling of compressed steam, which significantly reduces the steam

* Corresponding author.

required as well as the size of the boiler and condenser. The relatively low investment and operating cost of MED-TVC, due to the simplicity of the steam ejector, is an advantage over the MED-MVC system [8,9].

Despite its limited capacity (less than 5,000 m^3/d), the MED-MVC operates without a descending condenser and therefore without cooling water [10]. However, both systems are compatible with power controlled by CSP (concentrated solar power plants).

In this work, investigative analyzes are carried out for different MED techniques for a small capacity (350 m^3/d) using solar energy. Four different systems are studied and analyzed. Our systems use the rest of the exhaust energy from a Rankine organic cycle solar turbine to drive the MED process. Therminol VP-1 heat transfer oil (HTO) [11] and heat transfer fluid are used for the indirect generation of steam. The objective of this comparison is to define the most economical and profitable MED configuration to be implemented with solar energy. The software package [12] is used to simulate the different MED systems.

The aim of this work may be concluded into these points:

- Analysis and comparison of the limits of design and use of solar energy techniques for the different MED process configurations (MED-BF, MED-FF, MED-FFH MED-PF).
- Study the impact of increasing the number of evaporators on performance and the impact of varying other process parameters.

2. Organic Rankine cycles with solar energy for desalination

The technology of organic Rankine cycles is not new. It represents a very interesting option for producing solar electricity on a small scale. In fact, this configuration was the subject of study by the construction of an ORC Saguaro parabolic plant with a capacity of 1 MW [13]. The POWERSOL project (mechanical power generation based on solar heat engines), focuses on the technological development of a solar ORC to power an RO desalination unit. Fig. 1 shows a schematic diagram of the process configuration implemented by [14].

An experiment was carried out by Manolakos et al. [15] to study a Rankine solar cycle based on CO_2. The system uses cogeneration of heat and electricity, the thermal energy is recovered to be reused. According to the studies the solar ORC gives an interesting efficiency and this with different organic working fluids [15].

A laboratory performance evaluation of a low-temperature solar ORC system coupled to an RO desalination system was the subject of studies carried out by Zhang et al. [16]. The refrigerant (R134a) is evaporated via the thermal energy recovered by a network of solar heaters. The superheated steam is then sent to a regulator to produce mechanical work and to drive the pump to another pressure of the RO [16].

3. Solar MED process techniques description

3.1. MED process configurations

MED processes use a horizontal tube, the evaporative condensers are falling film and in a series arrangement, the production is done by repetitive stages and cycles (evaporation/condensation), stage after stage, temperature and pressure fall progressively. Technically, the number of stages or effects is limited by the temperature difference between the inlets temperatures of steam and seawater as well as the minimum temperature difference defined for each effect [17,18].

There are different seawater supply schemes for the supply of evaporators, mainly forwards, backwards, parallel and mixed systems [19]. In the MED-FF (forward feed arrangement), shown in Fig. 2, in this configuration the feed and vapor enter the effects and flow in the same direction and water is supplied to the first effect having the highest temperature after leaving the lower condenser.

In MED-BF (rear feed arrangement), shown in Fig. 3, the feed water is directed from the final condenser to the last effect (from the lowest temperature). The brine leaving the first effect is blown down to the sea, in this configuration, the supply and the steam entering the effects have opposite flow directions.

In the MED-PF (parallel power arrangement), shown in Fig. 4, the flow leaving the condenser is divided in a similar

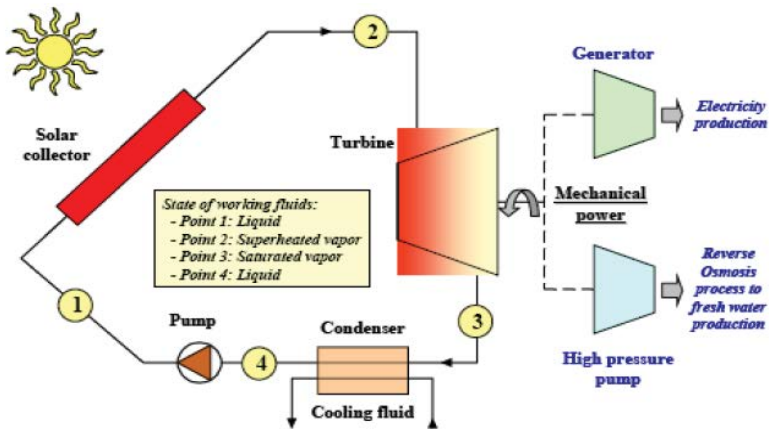

Fig. 1. POWERSOL – A solar-heated Rankine cycle drives either a generator or the high-pressure reverse osmosis pump [12].

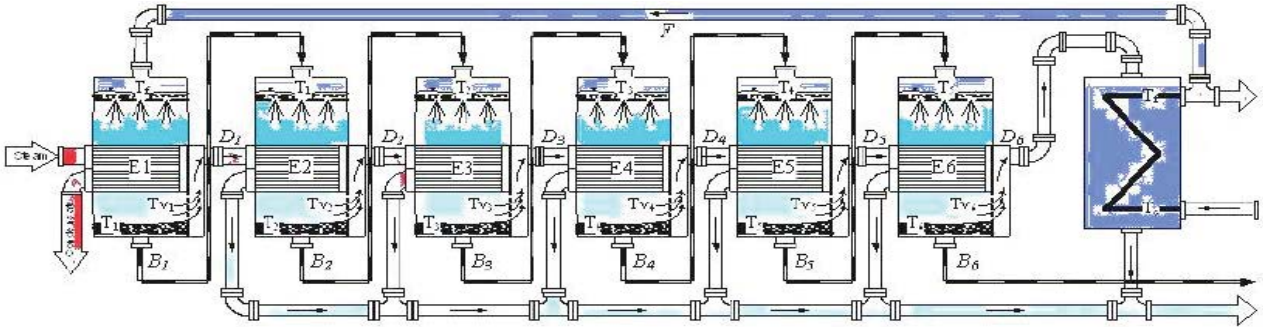

Fig. 2. MED-FF (forward feed configuration).

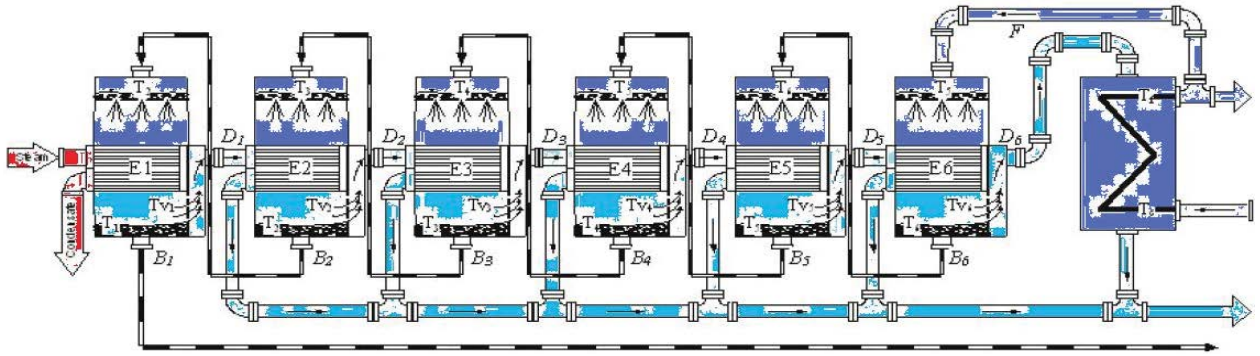

Fig. 3. MED-BF (forward feed configuration).

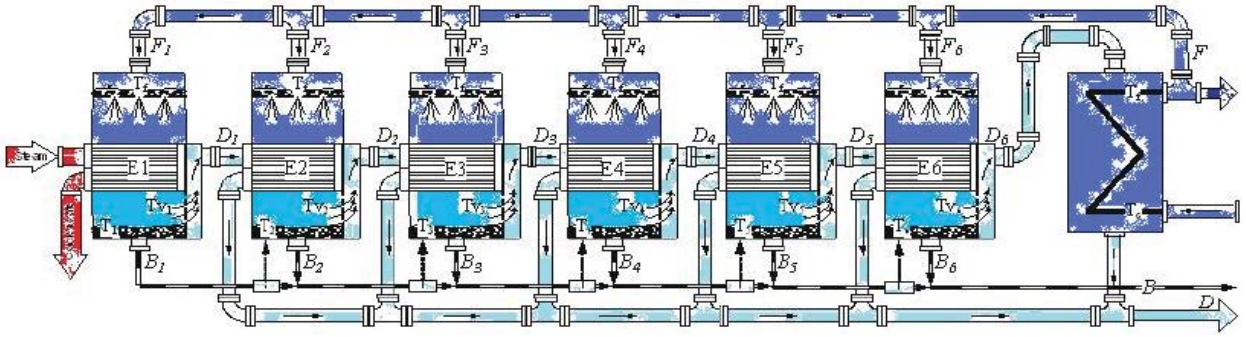

Fig. 4. MED-PF (forward feed configuration).

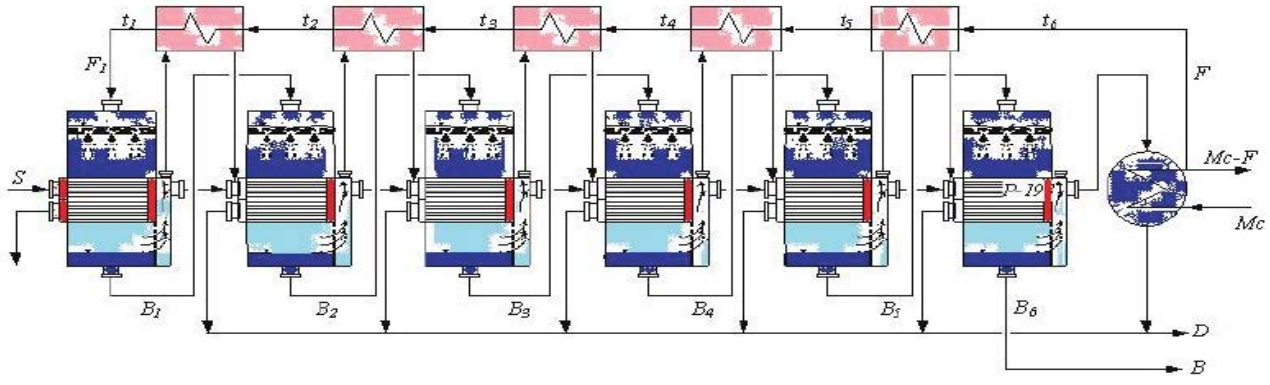

Fig. 5. MED-FFH (forward feed configuration with feedwater heaters).

way for each effect [19]. The choice of one of these supply arrangements directly affects the performance of the MED desalting system. The steam flow produced by each effect, the arrangement of the evaporator, the energy required for pumping, the gain ratio (distillate/heating steam), the ratio of cooling water to the distillate and the surface area of heat transfer required for effects [19].

For the MED-FFH (forward feed configuration with feed-water heaters), shown in Fig. 5, the cooling water condenses in the end condenser and a part (cooling water) is recycled to the supply after having undergone a pretreatment.

3.2. Solar desalination with different MED configuration

There are at least two methods for combining a thermal solar energy cycle with MED processes. In this work, we aim to study the use of the Rankine solar cycle for desalination and the production of electricity by using the exhaust steam of the turbine to operate the first effect.

The studied process consists of two circulation pumps, a solar collector field parabolic trough collector (PTC), a boiler heat exchanger (BHX), a turbine expansion vessel, a regeneration recuperator and overheating and a MED with 12 effects. The role of the added turbines and recuperators is the regeneration of electricity and energy. Fig. 6 shows a schematic diagram of the processing units. Fig. 7 is an example of the solar desalination system used on MATLAB-SimuLink for the MED-PF configuration.

4. Model of exergy, cost, and thermo-economic analysis

4.1. PTC collector

Based on the characteristic curve of the solar collector and the solar irradiance, its instantaneous efficiency is determined. The efficiency of the PTC at medium-high temperature is described by the equations below [20]:

$$\eta_{col} = \eta_0 - a_1\left(T_{co} - T_{amb}\right) - a_2\left(\frac{T_{co} - T_{amb}}{G_b}\right) - a_3\left(\frac{T_{co} - T_{amb}}{G_b}\right)^2 \quad (1)$$

where $a_1 = 4.5 \times 10^{-6}$, $a_2 = 0.039$, $a_3 = 3 \times 10^{-4}$, optical efficiency $\eta_0 = 0.75$ and operating temperature, °C > 170–400°C.

The area is deduced from the energy balance equation of the collector as a function of its efficiency:

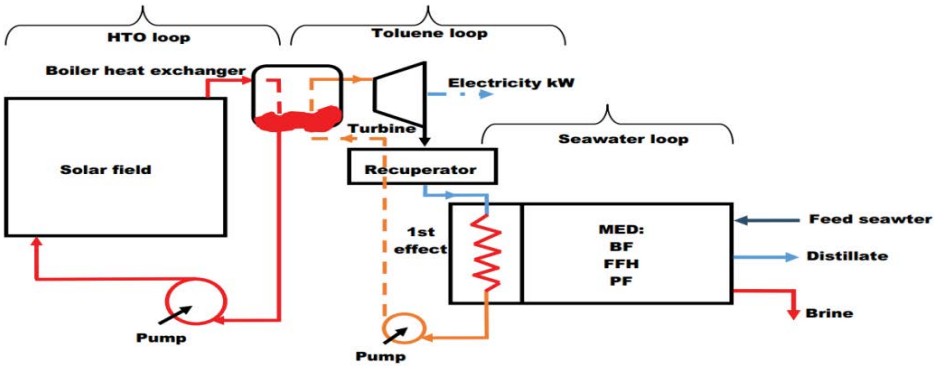

Fig. 6. A schematic diagram of solar MED components for desalination and power generation.

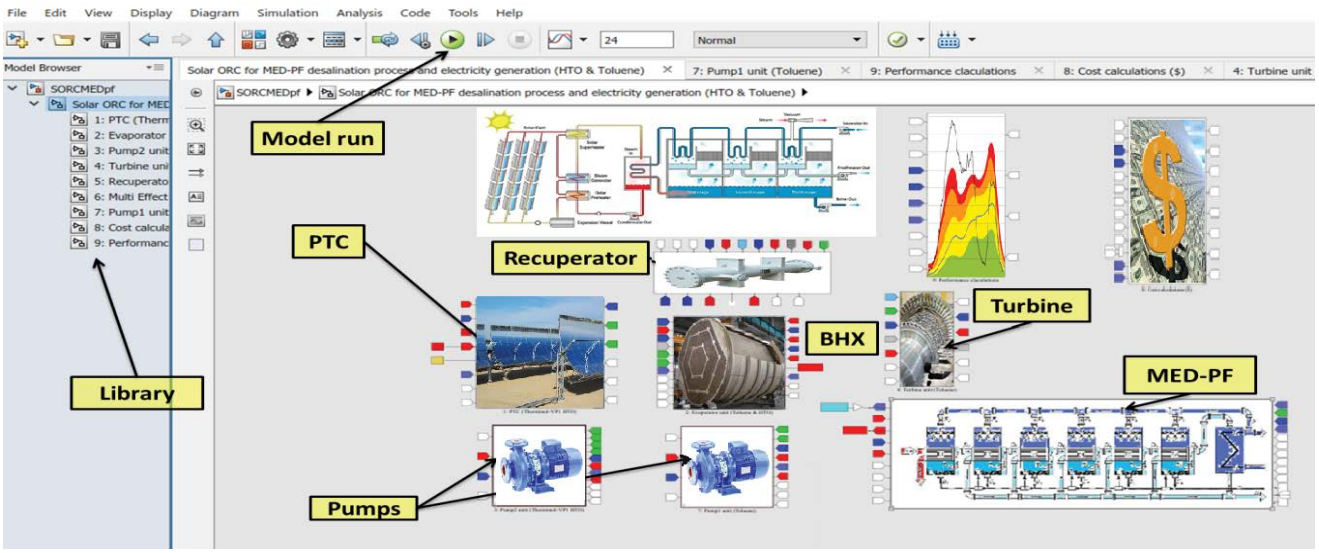

Fig. 7. Example of SDS for the MED-PF desalination process assisted by an organic solar Rankine cycle [10].

$$A_{\text{col}} = \frac{Q_u}{\eta_{\text{col}} G_b} \tag{2}$$

where (Q_u) is the useful thermal power, (G_b) is the normal solar radiation (W/m^2) at the surface of the A_{col} collector. The useful energy is deduced by the following equation:

$$Q_u = \dot{m}^*_{\text{col}} \times \Delta h \tag{3}$$

4.2. Exergy analysis

Exergy is destroyed due to irreversibility taking place in any process, which manifests itself in entropy creation or entropy increase. The general form of the exergy is defined by the following equation [21].

$$\text{Ex}_2 - \text{Ex}_1 = \text{Ex}_q + \text{Ex}_w + \text{Ex}_{f0} - \dot{I} \tag{4}$$

In steady state condition:

$$\text{Ex}_2 - \text{Ex}_1 = 0 \tag{5}$$

$$0 = \text{Ex}_q + \text{Ex}_w + \text{Ex}_{f0} - \dot{I} \tag{6}$$

The equations below define the exergetic destruction rate (kW) in the solar collector [22]:

$$\dot{I}_{\text{collector}} = A_{\text{col}} \times G_b \times \left(1 + \frac{1}{3}\left(\frac{T_{\text{amb}}}{T_{\text{sum}}}\right)^4 - \frac{4}{3}\left(\frac{T_{\text{amb}}}{T_{\text{sum}}}\right)\right) + \dot{m}_{\text{col}}\left[h_i - h_0 - T_{\text{amb}}\left(s_i - s_0\right)\right] \tag{7}$$

In this study the recommendation of Bejan et al. [23] is used (T_{sun} = 6,000 K).

$$\dot{I}_{\text{collector}} = \dot{m}\left[\Delta h_{i-0} - T_{\text{amb}} \times \Delta s_{i-0}\right] - \dot{W}_{\text{turbine}} \tag{8}$$

$$\dot{I}_{\text{rec,cond}} = \dot{m}_{\text{hot}}\left[\Delta h_{i-0} - T_{\text{amb}} \times \Delta s_{i-0}\right]_{\text{hot}} + \dot{m}_{\text{cold}}\left[\Delta h_{i-0} - T_{\text{amb}} \times \Delta s_{i-0}\right]_{\text{cold}} \tag{9}$$

$$\dot{I}_{\text{pump}} = \dot{m}\left[\Delta h_{i-0} - T_{\text{amb}} \times \Delta s_{i-0}\right] - \dot{W}_{\text{pump}} \tag{10}$$

$$\dot{I}_{\text{MED}} = \Delta \dot{\text{E}}\text{x}_{\text{stream}} = +\dot{W}_{\text{pumps}} - \dot{W}_{\text{turbine}} + \dot{\text{E}}\text{x}_f + \dot{\text{E}}\text{x}_b + \dot{\text{E}}\text{x}_d \tag{11}$$

Sea water heat for each stream [24]:

$$h_{f,d,b} = h_0 + \left(A \times T + \frac{B}{2} \times T^2 + \frac{C}{3} \times T^3 + \frac{D}{4} \times T^4\right) \tag{12}$$

where;
$h_0 = 9.6296s - 0.4312402s^2$
$A = 4{,}206.8 - 6.6197s + 1.2288 \times 10^{-2}s^2$
$B = -1.1262 + 5.4178 \times 10^{-2}s - 2.2719 \times 10^{-4}s^2$
$C = 1.2026 - 5.3566 \times 10^{-4}s + 1.8906 \times 10^{-6}s^2$
$D = 6.8774 \times 10^{-7} + 1.517 \times 10^{-6}s - 4.4268 \times 10^{-9}s^2$

The equation of physical exergy for saline stream is:

$$\dot{\text{E}}\text{x}_{\text{ph}} = \dot{m}\left(\begin{matrix} C_P\left(T,S\right) \times \left(T - T_0\right) \\ \times C_P\left(T,S\right) \log \dfrac{T}{T_0} \end{matrix}\right) \quad (T_0 \text{ is reference temperature}) \tag{13}$$

The energy stream is calculated according to the following equation:

$$\dot{\text{E}}\text{x}_{\text{ch}} = \dot{m}\left(\begin{matrix} N_{\text{mol}}\left(s, M_w, M_s\right) \times 10^{-3} \times 8.314 \\ \times T_0\left\{-X_w \times \log X_w - X_s \times \log X_w\right\} \end{matrix}\right) \tag{14}$$

A total stream exergy rate is calculated by:

$$\dot{\text{E}}\text{x}_{\text{total}} = \dot{\text{E}}\text{x}_{\text{ph}} + \dot{\text{E}}\text{x}_{\text{ch}} \tag{15}$$

With

$$X_w = \frac{N_{\text{pure}}\left(S, M_w\right)}{N_{\text{mol}}\left(S, M_w, M_s\right)} \tag{16}$$

$$N_{\text{pure}} = \frac{\left(1{,}000 - S\right)}{M_w} \tag{17}$$

$$X_s = \frac{N_{\text{salt}}\left(S, M_w\right)}{N_{\text{mol}}\left(S, M_w, M_s\right)} \tag{18}$$

$$N_{\text{salt}}\left(S, M_s\right) \tag{19}$$

$$N_{\text{mol}} = N_{\text{pure}} + N_{\text{salt}} \tag{20}$$

The exergy efficiency is performed based on the following relation:

$$\rho_{\text{ex}} = 1 - \frac{\dot{I}_{\text{total}}}{\dot{\text{E}}\text{x}_{in}} \tag{21}$$

4.3. Cost and thermo-economic analysis

The life of the plant (LTP) is fixed at 20 y, analyzes of the investment, operating and maintenance costs are carried out for each part of the desalination unit.

Tables 1 and 2 illustrate the investment capital and operating and maintenance costs (ICCO&M) [28].

5. Specifications and design parameters

The operating conditions considered for the two systems are assumed for Morocco (SAFI) one of the Mediterranean countries (SAFI: latitude [°] = 32.283,

Table 1
Costs for Solar Organic Rankine cycle equipment

Process step	ICC	O&M	TCC	Z, \$/h	Reference
Solar field	$150 \times (A_{col})^{0.95}$	$15\% \times (ICC_{col})$	$(A_f \times (ICC + O\&M)_{col})$	$(TCC_{col})/8{,}760$	[28]
Condensers	$150 \times (A_{cond})^{0.8}$	$25\% \times (ICC_{cond})$	$(A_f \times (ICC + O\&M)_{cond})$	$(TCC_{cond})/8{,}760$	[28]
Steam turbine	$4{,}750 \times (W_t)^{0.75}$	$25\% \times (ICC_t)$	$(A_f \times (ICC + O\&M)_t)$	$(TCC_t)/8{,}760$	[28]
Pump	$3{,}500 \times (W_p)^{0.47}$	$25\% \times (ICC_p)$	$(A_f \times (ICC + O\&M)_p)$	$(TCC_p)/8{,}760$	[28]

Table 2
Costs parameters for MED

Parameter	Correlation	Reference
Interest rate, %	5	[14]
Plant life time, (y)	20	[30]
Amortization factor, (1/y)	$A_f = \frac{i(1+i)^{LT_p}}{(1+i)^{LT_{p-1}}}$	[29]
Direct capital costs, (\$)	$DCC = 9 \times 10^5$	[29]
Annual fixed charges, (\$/y)	$AFC = A_f \times DCC$	[29]
Annual heating steam cost, (\$/y)	$AHSC = \frac{SHC \times L_s \times LF \times M_d \times 365}{1{,}000 \times PR}$; $SHC = \frac{1.466}{MkJ}$	[29]
Annual electric power cost, (\$/y)	$AEPC = SEC \times SPC \times LF \times M_d \times 365$; SEC = 0.06 \$/kWh	[29]
Annual chemical cost, (\$/y)	$ACC = SCC \times LF \times M_d \times 365$; SCC = 0.025 \$/m^3	[29]
Annual labor cost, (\$/y)	$ALC = SLC \times LF \times M_d \times 365$; SLC = 0.1 \$/m^3	[29]
Total annual cost, (\$/y)	$TAC_{MED} = AFC + AHSC + AEPC + ACC + ALC$	[29]
Operating and maintenance costs, (\$)	$OMC_{MED} = 0.02 \times DCC$	[29]
Hourly operating and maintenance costs in [\$/h]	$Z_{MED}^{IC\&OM} = \frac{OMC_{MED} \times A_f + AFC}{8{,}760}$	[29]
Total plant costs, (\$/y)	$TPC = TCC_{col} + TCC_{bhx} + TCC_{rec} + TCC_p + TCC_t + TAC_{MED}$	[29]
Total water price (\$/m^3)	$AWP = TPC/(D_p \times 365 \times LF)$	[29]

longitude [°] = –9.233, altitude [m] = 45). Fig. 8 presents the data which is extracted via the "METENORM software".

- The distilled product is set at 350 m^3/d, the inlet seawater supply temperature is 22°C with a salinity ratio of around 40,000 mg/kg. The output brine flow temperature is assigned to 43°C where, the number of effects is fixed at 12 effects and the brine purge the salinity ratio is fixed at 72 g/kg.
- Solar radiation and ambient temperature would be fixed as the previous technique (260 W/m^2 and 23°C).
- The manifold outlet temperature is maintained at 350°C to keep the saturated steam (toluene) entering the first stage of the turbine unit in the range of 200°C [25].
- The temperature of the condensed steam will be maintained at 70°C, to obtain the Top Steam Temperature (TST) at 75°C.
- The efficiency of turbines, generators, recuperators and pumps is respectively set at 85%, 93%, 85% and 75%.
- PTC configuration and design specifications are adjusted according to LS-3 type [26,27]
- LTP is the lifetime of the factory is fixed at 20 y.

Table 3 shows the design points selected for all techniques.

6. Results and discussions

6.1. Data results for MED systems (different configurations)

In this part, we present a detailed comparison of different MED power configurations. The results are illustrated in Table 4.

6.2. Interpretation and analysis of results

Table 4 shows that the MED-PF system gives relatively better results. MED-FFH comes just after and MED-BF comes last. The MED-FF system shows significant differences compared to the other systems, its low energy and thermo-economic performance makes it not applicable. Also, the MED-BF is very surpassed by the performances obtained by MED-PF and MED-FFH. For these reasons, MED-FF and MED-BF are eliminated from this comparison. MED-FFH is a little less efficient than MED-PF. In fact MED-PF requires less surface area of solar collectors (A_{col}-MED-PF is 9.5% less), and therefore a better installation cost (PTC) and low maintenance cost. The total area of A_{eff} effects is lower for MED-FFH, but if we add the

area of the heaters (A_{fh} = 100.7 m²), we will have a total of 2495.7 m² for MED-FFH against 2466 m² for MED-PF, which adds another advantage to the MED-PF configuration. The gain ratio (GR) of the MED-PF is higher than that of the MED-FFH (1.966 against 1.779) which is justified by the low vapor flow rate necessary for the operation of the MED-PF (2.06 against 2.28 kg/s). The results show that the MED-PF is the most reliable and efficient configuration, based on several key indicators and parameters such as the total water price (TWP, $/m³), A_{eff} (m²) and A_{col} surface (m²), the exergy balance, the GR, and other criteria as shown in Table 4.

Table 3
Design points retained for all of the techniques

Design points	MED
G_b, W/m²	260
T_{amb}, °C	23
T_{co}, °C	350
η_t, %	85
η_g, %	93
η_p, %	75
Seawater – condenser effectiveness, %	80
Recuperator effectiveness, %	85
Boiler heat exchanger effectiveness, %	80
Boiler inner tube diameter	0.0128
Boiler outer tube diameter, m	0.0130
T_{sea}, °C	22
T_{steam}, from boiler	200
T_b, °C	43
TST to the MED, °C	75
Feed salinity, ppm	40,000
Brine blow down salinity, ppm	72,000
Number of effects	12
Product mass flow rate, kg/s	4.051
Solar field mass flow rate per loop, kg/s	1
Plant life time, y	20
Power generation cost, $/kWh	0.06

6.3. Influence of the variation of the parameters (MED-PF)

Fig. 9 shows that by varying the seawater temperature from 10°C to 35°C with an interval of 5°C, the tendency of the T_{wp} ($/m³) decreases to reach a minimum value around 20°C, before growing. The increase in the temperature (T_{sea}, °C) of the seawater reduces the sensible heat necessary to reach the point of evaporation. However, the increase in the cooling water mass flow becomes necessary to compensate for the effect of the T_{sea} temperature increase, which subsequently explains the increase in TW when T_{sea} exceeds the optimum zone of about 20°C.

In Fig. 10 we notice that the increase in the number of effects reduces the TWP and increases the performance ratio (PR) which constitutes an advantage. The MED-PF configuration presents the most advantageous PR followed by the MED-FFH. However, the other configurations remain less competitive. Note that the advantage of MED-PF over MED-FFH is maintained when the number of effects is greater than 10, but if it is less than 8 effects, the MED-PF configuration becomes more competitive. This tilting zone is identified in Fig. 10 by a green highlight. Figs. 11 and 12 show that the increase in the daily production of distilled seawater will systematically increase the specific power consumption SPC (kWh/m³) which is explained by the effect of the increase in pumping costs, and the 'increased cooling flow required. But this increase is compensated in terms of global specific cost which decreases under the effects of invariable fixed costs.

As shown in Fig. 13 the increase in daily desalinated water productivity (m³/d) reduces the specific thermo-economic cost ($/GJ). This variation is the result of the effect of the GR of the system and of the effect of the exergy flow of the product. In fact, the increase in the exergy of the product implies a drop in the thermo-economic cost.

Figs. 14–16 show the effect of evaporators number and steam temperature on based (TSC), on the SDMED-PF technique. The results found relate to our SDMED-PF case study

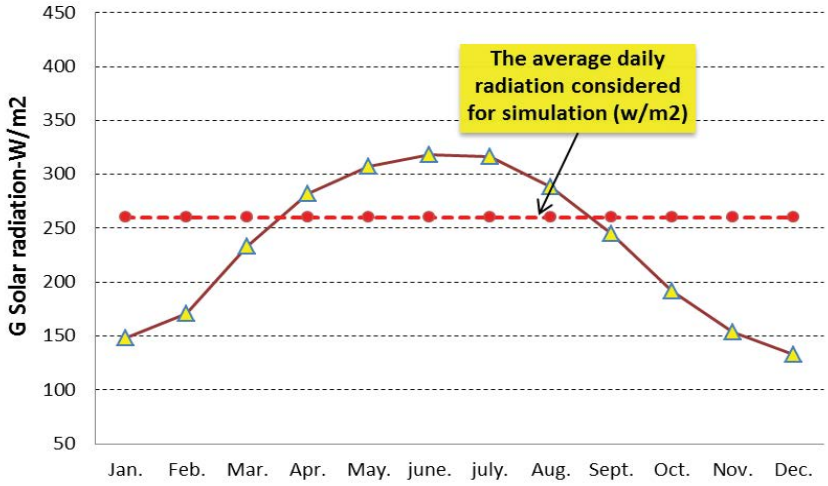

Fig. 8. A global solar radiation data of SAFI (Morocco).

Table 4
Results for MED operated by toluene and HTO fluids

Parameter		MED-BF	MED-FF	MED-FFH	MED-PF
Solar collector field	Total solar field area A_{col}, m^2	6.064	13.480	6.205	5.613
	Solar field flow rate M_{col}, kg/s	2.332	5.183	2.1	2.158
	Solar field renumber	2.769×10^4	2.769×10^4	1.919×10^4	2.769×10^4
	No. of collectors (LS-3)/no. of loops	4/1	24/5	11/2	5/1
	Solar field width w_{col}, m	26.81	26.81	30.47	26.81
	Solar collector thermal efficiency η_{col}, %	69.9	69.9	69.9	69.9
	Exergy destruction rate, kW	999.4	2206	1.041	894.6
	Exergy inlet rate, kW	1.499	3.331	1.534	1.363
	Cost stream to BHX, $/GJ	3.434	3.29	3.602	3.449
Boiler heat exchanger unit	Area, m^2	2.932	6.517	4.706	2.714
	Outlet HTO temperature, °C	130.7	130.7	95.06	130.7
	Exergy destruction rate, kW	184.4	409.9	163.6	170.7
	Cost stream to turbine, $/GJ	2.12×10^{-3}	1.436×10^{-3}	2.346×10^{-3}	0.928×10^{-3}
	Cost stream to pump, $/GJ	3.434	3.29	3.602	3.449
Turbine unit	Power developed, kW	239.5	532.3	245.2	221.7
	Outlet temperature, °C	81.6	81.6	81.6	81.6
	Exergy destruction rate, kW	90.97	202.2	93.07	84.21
	Cost of power, $/GJ	3.075	2.518	3.058	3.134
	Cost stream to recuperator, $/GJ	2.12×10^{-3}	1.436×10^{-3}	2.346×10^{-3}	0.953×10^{-3}
Recuperator unit	Power rejected, kW	25.23	56.07	25.81	23.35
	Area, m^2	3.088	3.753	1.727	1.563
	Top Steam Temperature, °C	71.86	71.86	71.86	71.86
	Preheated stream temperature, °C	75.87	75.87	75.87	75.87
	Cost stream to BHX, $/GJ	2.528×10^{-2}	3.388×10^{-2}	5.868×10^{-2}	6.561×10^{-2}
	Cost stream to MED, $/GJ	2.12×10^{-3}	1.436×10^{-3}	2.346×10^{-3}	0.953×10^{-3}
Rankine pump unit	Power, kW	1.144	2.543	1.171	1.059
	Exergy destruction rate, kW	483	1.072	0.494	0.446
	Cost stream to recuperator, $/GJ	8.188×10^{-2}	5.652×10^{-2}	7.857×10^{-2}	8.366×10^{-2}
HTO pump unit	Power, kW	1.786	4.078	1.565	1.650
	Exergy destruction rate, kW	0.906	2.088	0.663	0.836
	Cost stream to PTC, $/GJ	3.578	3.385	3.826	3.599
MED section (12 effects)	M_d, kg/s	4.051	4.051	4.051	4.051
	M_f, kg/s	9.115	9.115	9.115	9.115
	M_{cw}, kg/s	2.712	2.712	2.712	2.712
	M_s, kg/s	2.226	4.947	2.277	2.06
	T_f, °C	38.16	38.16	38.16	38.16
	T_d, °C	26.04	26.04	26.04	26.04
	TBT, °C	70.19	70.19	70.19	70.19
	TVT, °C	69.38	69.38	69.38	69.38
	TFT, °C	38.16	38.16	65.34	38.16
	Condenser area A_{cond}, m^2	42.63	42.63	42.63	42.63
	Total effects area A_{eff}, m^2	2.353	5.203	2.395	2.466
	Total feed heaters area A_{fh}, m^2	–	–	100.7	–
	GR	1.82	0.819	1.779	1.966
	Exergy destruction rate, kW	1.719×10^4	1.823×10^4	1.731×10^4	1.714×10^4
	Product cost stream C_d, $/GJ	0.681	0.701	0.677	0.625
Performance and cost	STPC, kWh/m^3	7.027	7.514	7.047	1.126
	ZIC&OM, $/h	18.94	28.79	19.14	18.38
	UPC med.	1.298	1.393	1.301	0.940
	Total plant cost, $/y	2.101×10^5	2.883×10^5	2.117×10^5	1.654×10^5
	TWP, $/m^3	1.828	2.507	1.841	1.438

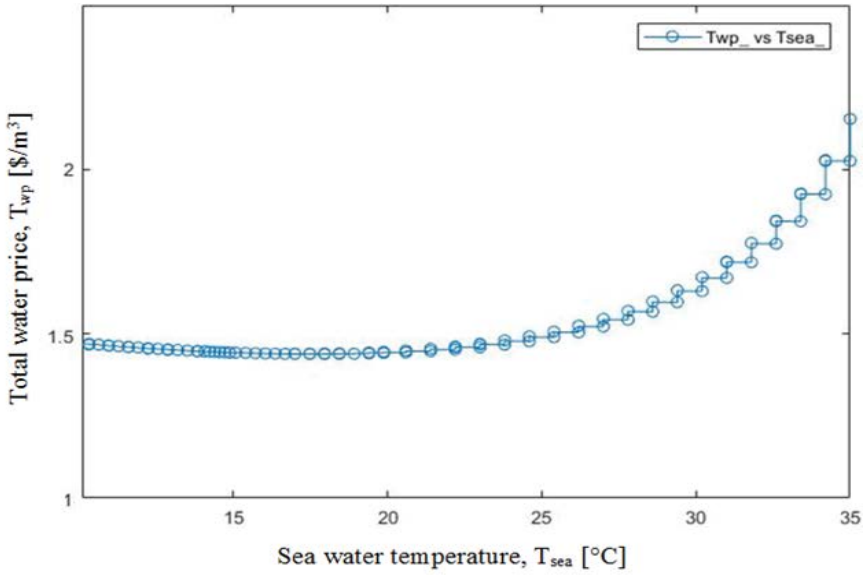

Fig. 9. Results for MED operated by toluene and HTO fluids.

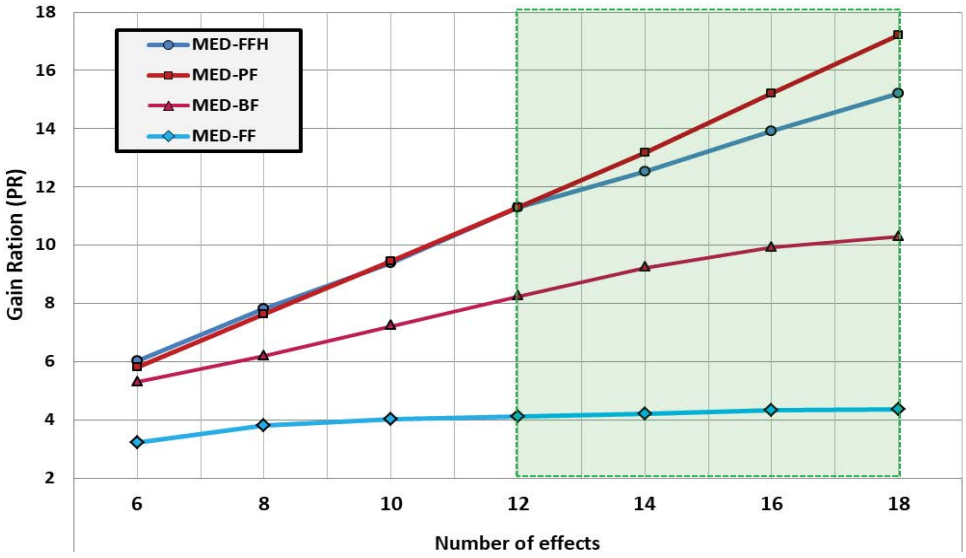

Fig. 10. The PR variations for different MED configurations with the variations of Neff.

(350 m^3/d). Fig. 16 shows that increasing the N_{eff} would decrease the TW ($/m^3). Indeed, the reduction in the mass flow rates of cooling water due to the increase in the number of effects (N_{eff}) would decrease the pumping power required, which explains the drop in SPC (kWh/m^3) and subsequently the decrease in TW ($/m^3) (production rate set at 350 m^3/d). We also observe a slight drop in TW as a function of TSC (°C).

The increase of N_{eff} and the decrease of TSC (Fig. 15) increase the thermo-economic cost CD ($/GJ). It is always recommended to keep CR in the optimal (low) zone, relative to the specifications of the desalination plant under consideration. The GR is also increased under the direct effect of N_{eff} (Fig. 14).

7. Conclusion

MED has the advantage of using a low temperature, so the energy consumed is available and lower. Reducing ΔT to less than 2°C–3°C greatly increases the heat transfer areas. The MED distillation process can use thermal solar energy instead of fossil fuel the techniques being developed are more and more competitive. In this work, we present an analysis and comparison study of four different configurations of MED desalination (BF, FF, FFH and PF) with a capacity of 350 m^3/d supplied by concentrated solar power plants (PTC solar collectors). The useful energy recovered from the sun via the solar collector is transferred to the first effect of the MED via the heat exchanger of the boiler, in

this technique a turbine unit is added to ensure the production of electricity. Toluene is chosen as the fluid instead of water because of its high performance across the turbine. Therminol VP-1 oil is used as a heat transfer fluid to operate the PTC. On the basis of the analysis carried out and the results found in this work, the following conclusions were drawn:

- To improve the performance of the MED technique, the increase in the number of effects up to 12–16 is important as well as the reduction of the top brine temperature (TBT) until reaching around 65°C. This allows to increase the gain ratio significantly lower the cost of specific production.

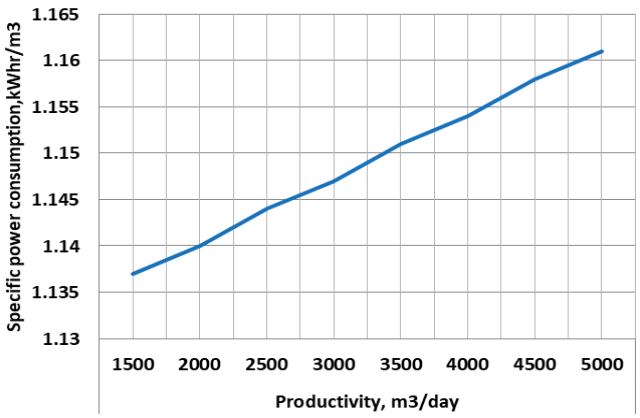

Fig. 11. Effect of production variation on SPC (kWh/m^3)-SMED-PF.

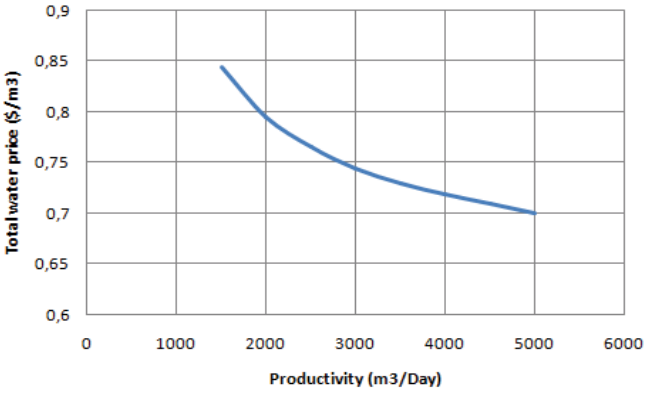

Fig. 12. Effect of production variation on TW ($/m^3)-SMED-PF.

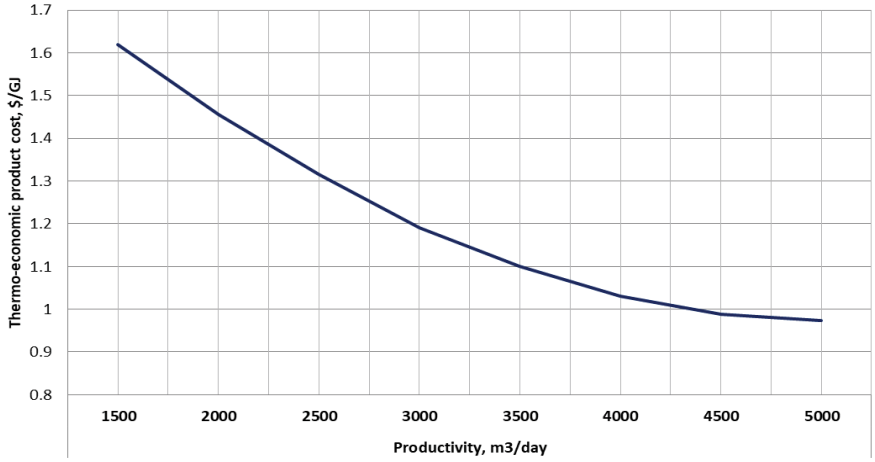

Fig. 13. Effect of productivity (m^3/d) on thermo-economic product cost ($/GJ)-SMED-PFF.

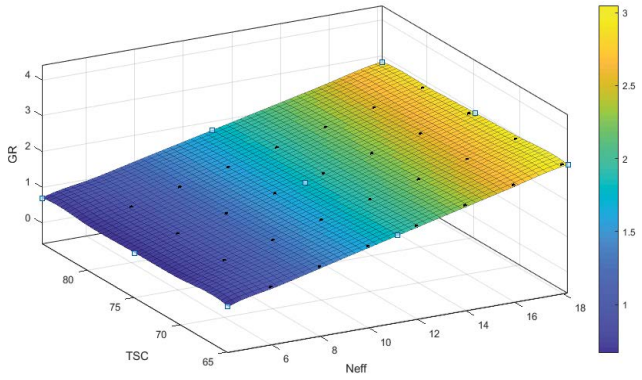

Fig. 14. Effect of evaporators number and steam temperature on based on GR.

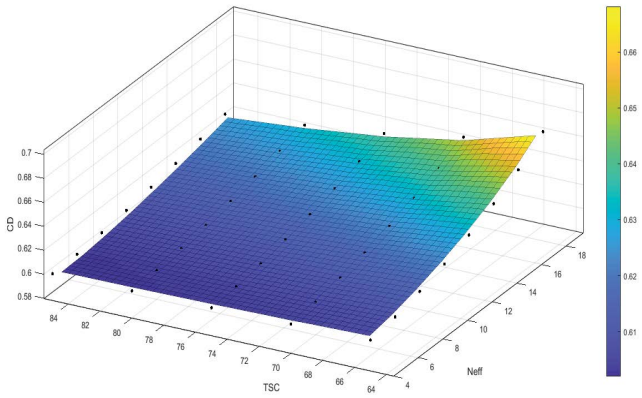

Fig. 15. Effect of evaporators number and steam temperature on based on CD, $/GJ.

- The MED-FF configuration records lower results compared to the rest of the configuration (MED-FFH-PF) following the overconsumption of energy used to increase the preheated feed stream to the fixed TBT.
- MED-BF is out of comparison due to its limited performance. Indeed, the increase in the salt level in the first effect which has the highest TBT presents technical difficulties.
- The MED-PF records the best results; it is more effective and becomes more effective when the number of effects is increased to 12–16 effects (Fig. 17). For MED-FFH the use of feed heaters improves the GR, at the same time it adds more complexity, capital cost and pumping energy, and more maintenance cost.
- The technique studied allows it to be developed and to produce electrical power, but this production depends on the quantity of distilled product and the operating conditions of the collector.
- The electricity produced by the systems could supply the needs of the pumps and the excess energy can be injected into the grid.

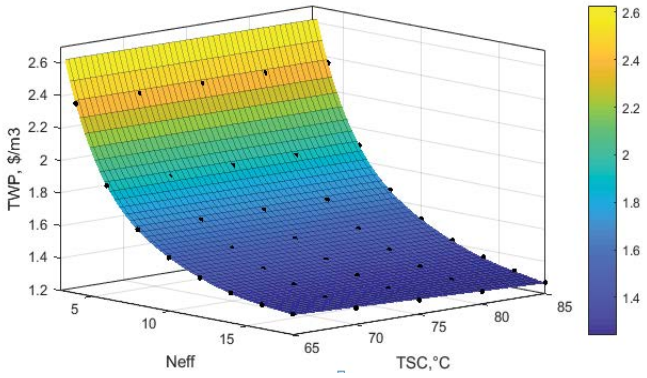

Fig. 16. Effect of evaporators number and steam temperature on based on TW, $/m³.

Symbols

A	—	Area, m²
A_{col}	—	Solar collector area, m²
$A_{effects}$	—	Effects heat transfer area, m²
A_f	—	Amortization factor, y
ACC	—	Annualized capital cost, $/y
BHX	—	Boiler heat exchanger
C	—	Cost, $
CC	—	Capital costs, $
PR	—	Performance ratio
C_d	—	Thermo-economic product cost, $/GJ
C_p	—	Specific heat capacity at constant pressure, kJ/kg K
DCC	—	Direct capital cost, $
Ex	—	Exergy rate, Kw
Ex_b	—	Brine blow down exergy rate, kW
Ex_{ch}	—	Chemical exergy rate, kW
Ex_d	—	Distillate exergy rate, kW
Ex_f	—	Flow exergy rate, kW
Ex_{in}	—	Exergy in, kW
Ex_{ph}	—	Physical exergy rate, kW
Ex_q	—	Exergy transfer, kW
Ex_{out}	—	Exergy out, kW
Ex_w	—	Exergy of work, kW
GR	—	Gain ratio, Md/Ms
G_b	—	Global solar radiation, W/m²
h	—	Enthalpy, kJ/kg
I	—	Exergy destruction rate, kW
ICC	—	Investment capital costs, $
IDCC	—	Indirect capital cost, $
i	—	Interest, %

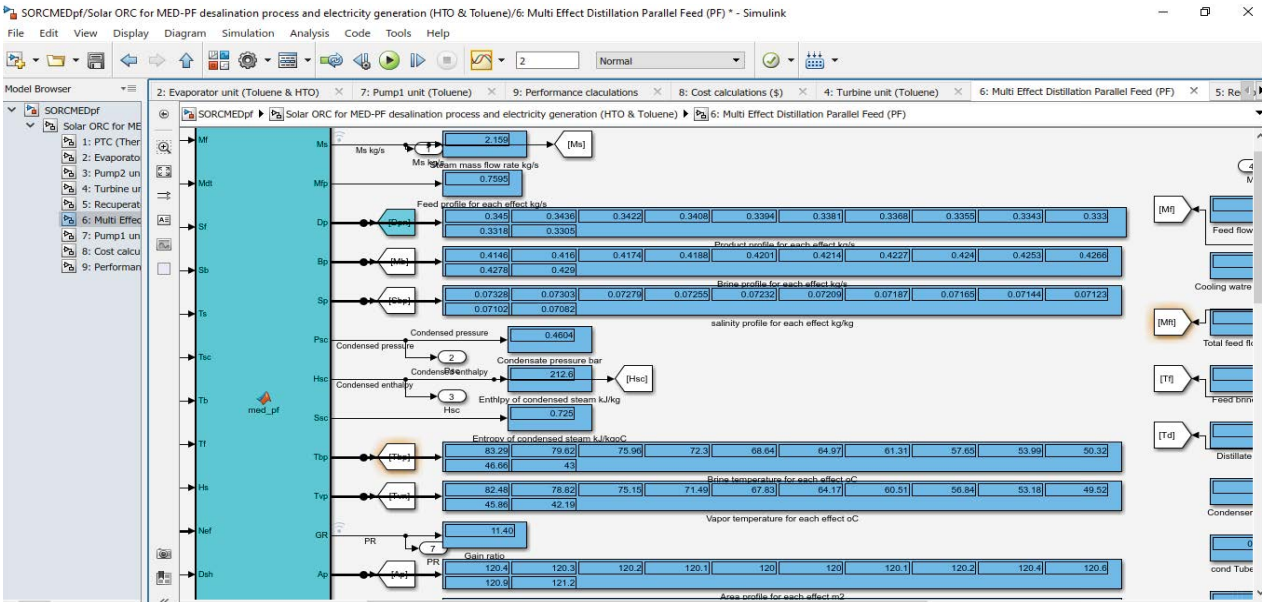

Fig. 17. Schematic display MED-PF under MATLAB-SimuLink.

LF	—	Load factor
LT	—	Life time, year
MED-BF	—	Multi-effect distillation backward feed arrangement
MED-FF	—	Multi-effect distillation forward feed arrangement
MED-FFH	—	Multi-effect distillation forward feed with feed heaters arrangement
MED-PF	—	Multi-effect distillation parallel/cross feed arrangement
MED-PF-TVC	—	Multi-effect distillation parallel/cross feed thermal vapor compression
M	—	Mass flow rate, kg/s
M_b	—	Brine mass flow rate, kg/s
M_d	—	Distillate mass flow rate, kg/s
M_s	—	Steam mass flow rate, kg/s
N_{eff}	—	Number of effects
N_{pure}	—	Number of moles of pure water, gmol
N_{salt}	—	Number of moles of salt, gmol
OC	—	Operating cost, $
P	—	Pressure, kPa
S	—	Salinity ratio, g/kg (ppm)
Sb	—	Brine blow down salinity ratio, g/kg
Sf	—	Feed seawater salinity ratio, g/kg
S-ORC	—	Solar organic Rankine cycle
SCC	—	Specific chemical cost, $/m^3
SEC	—	Specific electrical cost, $/kWh
SHC	—	Specific heating steam cost, $/MkJ
SLC	—	Specific labor cost, $/m^3
SPC	—	Specific power consumption, kWh/m^3
S	—	Specific entropy, kJ/kg °C
T	—	Temperature, °C
T_d	—	Distillate temperature, °C
T_{bn}	—	Last effect brine temperature, °C
T_{sea}	—	Seawater temperature, °C
TBT	—	Top brine temperature, °C
TDT	—	Top distillate temperature, °C
TSC	—	Top steam temperature, °C
TVT	—	Top vapor temperature, °C
T_{sun}	—	Sun temperature, 6,000 K
TCC	—	Total capital cost, $
TWP	—	Total water price, $/m^3
W_{turbine}	—	Turbine power, kW
W_{pump}	—	Pump power, kW
$X_{w,s}$	—	Fraction of water and salt contents
ZIC&OM	—	Total investment and operating and maintenance cost, $/h

Subscripts

amb	—	Ambient
av	—	Average
b	—	Brine
chm	—	Chemical
col	—	Collector
cond	—	Condenser
cw	—	Cooling water
d	—	Distillate product
f	—	Feed
i	—	In
MED	—	Multi effect distillation
o	—	Out of reference
p	—	Pump
rec	—	Recuperator
s	—	Salt
t	—	Turbine
w	—	Water
ORC	—	Organic Rankine cycle

References

[1] C. Karagiannis, P.G. Soldatos, Water desalination cost literature: review and assessment, Desalination, 223 (2008) 448–456.

[2] A. Lilane, D. Saifaoui, Y. Aroussy, S. Hariss, M. Oulhazzan, Experimental study of a pilot membrane desalination system: the effects of transmembrane pressure, Mater. Today:. Proc., 30 (2020) 970–975.

[3] L.P. Yang, T. Shen, B. Zhang, S.Q. Shen, K. Zhang, Exergy analysis of a solar-assisted MED desalination experimental unit, Desal. Water Treat., 51 (2013) 1272–1278.

[4] M. Moser, F. Trieb, J. Kern, H. Allal, N. Cottret, J. Scharfe, M.-L. Tomasek, E. Savoldi, The MED-CSD project: potential for concentrating solar power desalination development in Mediterranean countries, J. Sol. Energy Eng., 133 (2011) 031012, doi: 10.1115/1.4004352.

[5] M.A. Darwish, Technical aspects of reducing desalting water costs in distillation methods, Desalination, 72 (1989) 381–393.

[6] B. Milow, E. Zarza, Advanced MED solar desalination plants. Configurations, costs, future — seven years of experience at the Plataforma Solar de Almeria (Spain), Desalination, 108 (1996) 51–58.

[7] J. Jiang, H. Tian, M.X. Cui, L.J. Liu, Proof-of-concept study of an integrated solar desalination system, Renewable Energy, 34 (2009) 2798–2802.

[8] N.M. Al-Najem, M.A. Darwish, F.A. Youssef, Thermovapor compression desalters: energy and availability – analysis of single-and multi-effect systems, Desalination, 110 (1997) 223e38.

[9] Y. Aroussy, D. Saifaoui, A. Lilane, M. Tarfaoui, Thermo-economic simulation and analysis of a solar thermal cycle combined with two desalination processes by multi-effect distillation (MED, Mater. Today:. Proc., 30 (2020) 1027–1032.

[10] A.S. Nafey, H.E.S. Fath, A.A. Mabrouk, Thermoeconomic design of a multi-effect evaporation mechanical vapor compression (MEE–MVC) desalination process, Desalination, 230 (2008) 1–15.

[11] M.A. Sharaf, A.S. Nafey, L. García-Rodríguez, Thermo-economic analysis of solar thermal power cycles assisted MED-VC (multi effect distillation-vapor compression) desalination processes, Energy, 36 (2011) 2753–2764.

[12] A.S. Nafey, M.A. Sharaf, L. García-Rodríguez, A new visual library for design and simulation of solar desalination systems (SDS), Desalination, 259 (2010) 197–207.

[13] A.C. Mcmahan, Design & Optimization of Organic Rankine Cycle Solar-Thermal Powerplants, University of Wisconsin, Madison, 2006.

[14] L. García-Rodríguez, J. Blanco-Gálvez, Solar-heated Rankine cycles for water and electricity production: POWERSOL project, Desalination, 212 (2007) 311–318.

[15] D. Manolakos, G. Papadakis, S. Kyritsis, K. Bouzianas, Experimental evaluation of an autonomous low-temperature solar Rankine cycle system for reverse osmosis desalination, Desalination, 203 (2007) 366–374.

[16] X.R. Zhang, H. Yamaguchi, K. Fujima, M. Enomoto, N. Sawada, A feasibility study of CO_2-based Rankine cycle powered by solar energy, JSME Int J., Ser. B, 48 (2005) 540–547.

[17] A. Ophir, F. Lokiec, Advanced MED process for most economical sea water desalination, Desalination, 182 (2005) 187–198.

[18] M. Tunc, S. Sİsbot, Influence of seawater temperature on thermal efficiency of an integrated electric power generation and water desalination plant, Desal. Water Treat., 59 (2017) 82–88.

[19] M.A. Darwish, H. Abdulrahim, Feed water arrangements in a multi-effect desalting system, Desalination, 228 (2008) 30–54.
[20] M.A. Sharaf Eldean, A.M. Soliman, Study of using solar thermal power for the margarine melting heat process, J. Sol. Energy Eng., 137 (2014) 210041–2100413.
[21] K.W. Li, Applied Thermodynamics: Availability Method and Energy Conversion, CRC Press, 1995.
[22] F. Banat, N. Jwaied, Exergy analysis of desalination by solar-powered membrane distillation units, Desalination, 230 (2008) 27–40.
[23] A. Bejan, G. Tsatsaronis, M.J. Moran, Thermal Design and Optimization, Wiley, New York, 1995.
[24] A.S.M. Nafey, Design and Simulation of Seawater Thermal Desalination Plants, Doctoral Dissertation, University of Leeds, 1988.
[25] A.M. Delgado-Torres, L. García-Rodríguez, Comparison of solar technologies for driving a desalination system by means of an organic Rankine cycle, Desalination, 216 (2007) 276–291.
[26] A.M. Delgado-Torres, L. García-Rodríguez, Preliminary assessment of solar organic Rankine cycles for driving a desalination system, Desalination, 216 (2007) 252–275.
[27] J. Blanco, Technical Comparison of Different Solar-Assisted Heat Supply Systems for a Multi-Effect Seawater Distillation Unit, ISES Solar World Congress, 2003.
[28] N.G. Voros, C.T. Kiranoudis, Z.B. Maroulis, Solar energy exploitation for reverse osmosis desalination plants, Desalination, 115 (1998) 83–101.
[29] H.T. El-Dessouky, H.M. Ettouney, Fundamental of Salt Water Desalination, Kuwait University, Elsevier Science, 2002.
[30] A. Malek, M.N. Hawlader, J.C. Ho, Design and economics of RO seawater desalination, Desalination, 105 (1996) 245–261.